Mixed Ground-state in the Trinuclear Complex: $[Mn_3O(O_2CCCl_3)_6(H_2O)_3]$

Hui-Lien Tsai[a]* (蔡惠蓮), Tyn-Yih Jwo[a] (卓庭義), Chen-I Yang[a] (楊振宜), Ching-Shuei Wur[b] (吳清水), Gene-Hsiang Lee[c] (李錦祥) and Yu Wang[c] (王　瑜)
[a]*Department of Chemistry, National Cheng Kung University, Tainan 701, Taiwan, R.O.C.*
[b]*Department of Physics, National Cheng Kung University, Tainan 701, Taiwan, R.O.C.*
[c]*Instrumentation Center, College of Science, National Taiwan University, Taipei 106, Taiwan, R.O.C.*

The reaction of $[Mn_{12}O_{12}(OAc)_{16}(H_2O)_4]\cdot 4H_2O\cdot 2HOAc$ with Cl_3CCO_2H in dichloromethane leads to formation of mixed-valence trinuclear oxo-centered $[Mn_3O(O_2CCCl_3)_6(H_2O)_3]\cdot 2H_2O$ (**1**). Complex **1** crystallizes in two forms; the monoclinic and hexagonal systems. $[Mn_3O(O_2CCCl_3)_6(H_2O)_3]\cdot 3H_2O$ (**1a**) crystallizes in hexagonal, space group $P6_3/m$ (295 K) with a = 10.0741(1) Å, c = 22.8668(4) Å, and z = 2. $[Mn_3O(O_2CCCl_3)_6(H_2O)_3]\cdot 0.5C_6H_{14}$ (**1b**) crystallizes in monoclinic, space group $P2_1/n$ (150 K) with a = 11.8258(2) Å, b = 41.9370(5) Å, c = 25.9619(4) Å , β = 95.297(1)°, and z = 12. Complex **1** possesses an oxo-centered Mn_3O unit with peripheral ligands provided by bridging trichloroacetate and terminal H_2O groups. Each manganese ion is distorted octahedral, and consideration of overall charge of the trinuclear unit necessitates a mixed-valence $Mn^{II}Mn^{III}_2$ description. Magnetization measurement at 2.0 K up to 70 kG indicates the mixed ground state S = 3/2 and S = 1/2 for complex **1**. X-band EPR spectra measured at 4.0-100.0 K on polycrystalline sample of complex **1**. There is a transition centered at g ≈ 4, which decreases in intensity with increasing temperature. Also, there is a transition centered at g ≈ 2, which does not disappear with increasing temperature.

Keywords: Trinuclear manganese complex; Mixed-valence complex; Crystal structure; Magnetochemistry; Magnetic exchange coupling; EPR.

INTRODUCTION

The ground states in many trinuclear μ_3-oxo centered $Mn^{II}Mn^{III}_2$ complexes results from spin frustration.[1-10] By changing the ratio of exchange coupling constant in a Mn_3O complex, it is possible to stabilize the ground state with different total spin S_T for a $Mn^{II}Mn^{III}_2$ complex.[4,6] It has been reported that $[Mn_3O(O_2CCH_3)_6(py)_3]\cdot py$ (**2**) has an S = 3/2 ground state and $[Mn_3O(O_2CPh)_6(py)_2(H_2O)]\cdot 0.5CH_3CN$ (**3**) has an S = 1/2 ground state.[4] A mixed ground state complex, S = 3/2, 1/2 for $[Mn_3O(O_2CPh\text{-}3\text{-}Br)_6(py)_2(H_2O)]$ (**4**), has also been reported.[6] As subtle changes in the exchange interaction due to small changes in the structure within a complex, the spin of the ground state can change appreciably. Trinuclear mixed valence manganese complexes with only oxygen coordination, $[Mn_3O(O_2CR)_6(H_2O)_3]$, have not been the object of investigation to date. Here, the first only oxygen coordination structure of $[Mn_3O(O_2CCCl_3)_6(H_2O)_3]\cdot 2H_2O$ (**1**), which is a mixed ground state complex, will be described, together with the results of magnetic susceptibility studies.

EXPERIMENTAL SECTION

Materials

All chemicals and solvents were used as received; all preparations were performed under aerobic conditions. $[Mn_{12}O_{12}(OAc)_{16}(H_2O)_4]\cdot 2HOAc\cdot 4H_2O$ was synthesized as reported elsewhere.[11]

Synthesis

To a slurry of $[Mn_{12}O_{12}(OAc)_{16}(H_2O)_4]\cdot 2HOAc\cdot 4H_2O$ (0.6815 g, 0.365 mmol) in CH_2Cl_2 (60 mL) was added Cl_3CCO_2H (2.5044 g, 15.33 mmol). The mixture was stirred for 2 days and filtered to remove undissolved solid. Hexanes (100 mL) were added to the filtrate, and the solution was stored for 2 days at room temperature. The resulting crystals were filtered, recrystallized from CH_2Cl_2 solution layered by hexanes and gave mainly complex **1a**. The complex **1b** crystals were recrystallized from CH_2Cl_2 solution by hexanes vapor diffusion. The overall yield was ~65%. Selected IR data (cm^{-1}): 1671 (vs), 1618 (sh), 1365 (vs), 965 (w), 838 (s),

* Corresponding author. E-mail: hltsai@mail.ncku.edu.tw

748 (s), 691 (s), 555 (m), 511 (w), 458 (m). Anal. Calcd for $[Mn_3O(O_2CCCl_3)_6(H_2O)_3]\cdot 2H_2O$ (**1**): C, 11.58; H, 0.81. Found: C, 11.55; H, 0.81.

Physical Measurements

Infrared spectra were recorded on a Nicolet Magna-550 FTIR spectrophotometer as KBr pellets in the 400-4000 cm^{-1} region. EPR spectra were recorded on a polycrystalline sample at X-band frequency with a Bruker EMX-10 spectrometer, varying the temperature from 5.0 to 100.0 K. Variable temperature dc magnetic susceptibility measurements were collected on powdered samples (restrained in eicosane to prevent torquing) on a Quantum Design MPMS SQUID susceptometer equipped with a 7.0 Tesla magnet and operating in the range of 1.7-300.0 K. Variable temperature ac magnetic susceptibility measurements were carried out on a Quantum Design PPMS equipped with a 14.0 Tesla magnet and operating in the range of 1.8-400 K. Diamagnetic corrections were estimated from Pascal's constants[12] and subtracted from the experimental susceptibility data to obtain the molar paramagnetic susceptibility of the compound.

X-ray Crystallography

Data were collected on a SMART CCD using graphite monochromatized Mo-Kα radiation (λ = 0.71073 Å). The crystallographic data, data collections and structural refinement parameters for complexes **1a** and **1b** are summarized in Table 1. Selected bond distances and bond angles are presented in Tables 2 and 3 for complexes **1a** and **1b**, respectively. The complete bond distances and angles, atomic coordinates, and thermal parameters of complexes **1a** and **1b** are given as supplementary materials.

RESULTS AND DISCUSSIONS

Synthesis and structure

Complex **1** represents the first example of an Mn_3O (II,III,III), where each MnO_6 coordinates with acetate derivatives as bridging ligands and with three water as terminal ligands. Similar examples reported so far were with carboxylate ligands as bridging ligands with pyridine and/or water as terminal ligands. Complex **1a** crystallizes in hexagonal space group $P6_3/m$. The data were collected at 295 K. An ORTEP projection is shown in Fig. 1. The crystallographic C_3 axis is perpendicular to the Mn_3 plane and passes through central oxygen. The charge on the complex necessitates a mixed-valence $Mn^{II}Mn^{III}{}_2$ description; however, complex **1a** has im-

Table 1. Crystallographic Data for **1a** and **1b**

	1·3H_2O (**1a**)	**1**·0.5C_6H_{14} (**1b**)
Formula	$C_{12}H_{12}Cl_{18}Mn_3O_{19}$	$C_{15}H_{15}Cl_{18}Mn_3O_{16}$
Formula weight	1263.14	1252.17
Temperature/K	295 (2)	150 (1)
Crystal system	Hexagonal	Monoclinic
Space group	$P6_3/m$	$P2_1/n$
a/Å	10.0741 (1)	11.8258 (2)
b/Å	10.0741 (1)	41.9370 (5)
c/Å	22.8668 (4)	25.9619 (4)
β/^{0}		95.297 (1)
V/Å^3	2009.78 (5)	12820.5 (3)
Z	2	12
D_{calc}/g cm^{-3}	2.087	1.946
μ (Mo-Kα)/mm^{-1}	2.192	2.056
F(0 0 0)	1234	7344
Crystal dimensins/mm	0.40 × 0.25 × 0.10	0.35× 0.30 × 0.30
Reflections measured	14150	54261
Independent reflections	1584	22180
R_{int}	0.0458	0.0282
Goodness-of-fit on F^2	1.205	1.456
R^a (R_w)^b (I > 2σ (I))	0.0658 (0.1359)	0.0650 (0.1917)
R (R_w) (all data)	0.0765 (0.1417)	0.0783 (0.1988)
Maxium residual peak/e Å^{-3}	0.702	1.800
Minimum residual peak/e Å^{-3}	-1.145	-1.242

[a] $R = (\Sigma||F_O|-|F_C||) / \Sigma|F_O|$.
[b] $R_w = [\Sigma w(|F_O|-|F_C|)^2 / \Sigma w|F_O|^2]^{1/2}$.

Table 2. Selected Bond Distances (Å) and Angles (°) for Complex **1a**

Mn(1)-O(1)	1.9236(11)	Mn(1)-O(2)	2.017(8)
Mn(1)-O(3)	2.065(4)	Mn(1)-O(4)	2.077(4)
C(1)-O(3)	1.203(6)	C(1)-C(2)	1.561(6)
C(2)-Cl(1)	1.762(4)	C(2)-Cl(2)	1.766(4)
C(2)-Cl(3)	1.750(5)		
O(1)-Mn(1)-O(2)	179.2(2)	O(1)-Mn(1)-O(3C)	94.66(12)
O(2)-Mn(1)-O(3C)	85.9(2)	O(1)-Mn(1)-O(3)	94.66(12)
O(2)-Mn(1)-O(3)	85.9(2)	O(3C)-Mn(1)-O(3)	92.0(4)
O(1)-Mn(1)-O(4)	93.49(12)	O(2)-Mn(1)-O(4)	86.0(2)
O(3C)-Mn(1)-O(4)	171.9(2)	O(3)-Mn(1)-O(4)	87.4(2)
O(1)-Mn(1)-O(4C)	93.49(12)	O(2)-Mn(1)-O(4C)	86.0(2)
O(3C)-Mn(1)-O(4C)	87.4(2)	O(3)-Mn(1)-O(4C)	171.9(2)
O(4)-Mn(1)-O(4C)	91.9(3)	O(3)-C(1)-O(4A)	127.1(5)
O(3)-C(1)-C(2)	115.3(4)	O(4A)-C(1)-O(2)	117.5(4)
C(1)-C(2)-Cl(3)	108.7(3)	C(1)-C(2)-Cl(1)	111.8(3)
Cl(1)-C(2)-Cl(3)	105.9(2)	C(1)-C(2)-Cl(2)	108.5(3)
Cl(2)-C(2)-Cl(3)	110.2(3)	Cl(1)-C(2)-Cl(2)	108.8(2)
C(1)-O(3)-Mn(1)	131.0(4)	C(1B)-O(4)-Mn(1)	132.2(4)
Mn(1A)-O(1)-Mn(1)	120.0		

posed C_3 symmetry so that the three manganese ions are electronically equivalent and are assigned a formal oxidation state of $2^2/_3$. A bond valence sum analysis[13] was calculated in order to gain further evidence for the described oxidation state assignment in complex **1a**, and the value is close to 2.87 based on relative Mn-O bond distances, which is consistent with the formal oxidation state of complex **1a**. The Mn_3O triangle is an equilateral triangle, with Mn-Mn, Mn-μ_3-O and Mn-O (water) distances of 3.343, 1.9236 and 2.017 Å, respectively. The Mn coordination geometry is a slightly distorted octahedral with six oxygen atoms from bridging acetate groups and a terminal water ligand. The overall structure is thus of the common "basic carboxylate" type seen for many transition metals.[1-10]

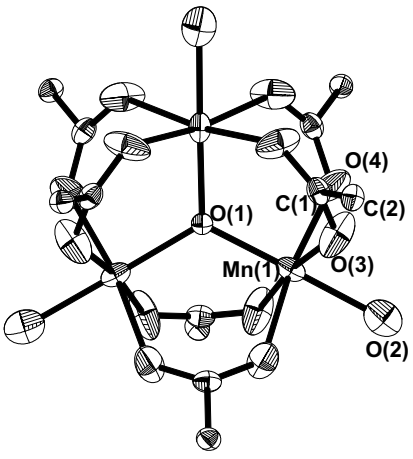

Fig. 1. Crystallographic Structure of $[Mn_3O(O_2CCCl_3)_6(H_2O)_3]\cdot 3H_2O$ (**1a**). Thermal ellipsoids at the 30% probability level. The Cl, H atoms and solvated molecules have been omitted for clarity.

However, complex **1b** was crystallized in monoclinic space group $P2_1/n$ and contained three independent Mn_3O units in the asymmetric unit. The metric parameters of the three molecules are compared in Table 3 and show a little difference. An ORTEP projection for one of three is shown in Fig. 2. The complex **1b** again possesses distorted octahedral metal geometries and approximates to C_{2v} symmetry but has no imposed elements. The O(1)-Mn distances are 1.847(3) Å for Mn(1), 1.833(3) Å for Mn(3), and 2.172(3) Å for Mn(2). The O(17)-Mn distances are 1.835(3) Å for Mn(4), 1.846(3) Å for Mn(6), and 2.182(3) Å for Mn(5). The O(33)-Mn distances are 1.843(4) Å for Mn(8), 1.842(3) Å for Mn(9), and 2.179(4) Å for Mn(7). The Mn coordination geometries are slightly distorted octahedrals with oxygen of the central triangle, four oxygen atoms from bridging trichoroacetate ligands and a terminal oxygen (H_2O). The average values for the Mn-O bond distances are 2.028 Å for Mn(1), 2.032 Å for Mn(3), 2.175 Å for Mn(2), 2.028 Å for Mn(4), 2.022 Å for Mn(6), 2.178 Å for Mn(5), 2.031 Å for Mn(8), 2.030 Å for Mn(9), and 2.164 Å for Mn(7). The Mn(1)…Mn(3) distance 3.264 Å is shorter than the Mn(1,3)…Mn(2) distances (3.430 and 3.438 Å). The Mn(4)…Mn(6) distance 3.259 Å is shorter than the Mn(4,6)…Mn(5) distances (3.452 and 3.442 Å). The Mn(8)…Mn(9) distance 3.266 Å is shorter than the Mn(8,9)…Mn(7) distances (3.427 and 3.459 Å). For all these

Table 3. Selected Bond Distances (Å) and Angles (°) for Complex **1b**

Distances					
Molecule A		Molecule B		Molecule C	
Mn(1)-O(1)	1.847(3)	Mn(6)-O(17)	1.846(3)	Mn(8)-O(33)	1.843(4)
Mn(1)-O(11)	1.960(4)	Mn(6)-O(30)	1.961(4)	Mn(8)-O(44)	1.973(4)
Mn(1)-O(5)	1.985(4)	Mn(6)-O(24)	1.981(4)	Mn(8)-O(45)	2.010(4)
Mn(1)-O(2)	1.998(4)	Mn(6)-O(20)	2.013(4)	Mn(8)-O(35)	2.005(4)
Mn(1)-O(7)	2.180(4)	Mn(6)-O(22)	2.168(4)	Mn(8)-O(47)	2.165(4)
Mn(1)-O(9)	2.200(4)	Mn(6)-O(32)	2.165(4)	Mn(8)-O(42)	2.192(4)
Mn(2)-O(3)	2.143(4)	Mn(5)-O(19)	2.166(4)	Mn(7)-O(34)	2.147(4)
Mn(2)-O(12)	2.153(4)	Mn(5)-O(29)	2.155(4)	Mn(7)-O(43)	2.138(4)
Mn(2)-O(15)	2.163(4)	Mn(5)-O(26)	2.142(4)	Mn(7)-O(39)	2.134(4)
Mn(2)-O(1)	2.172(3)	Mn(5)-O(17)	2.182(3)	Mn(7)-O(33)	2.179(4)
Mn(2)-O(10)	2.209(4)	Mn(5)-O(31)	2.184(4)	Mn(7)-O(41)	2.190(4)
Mn(2)-O(13)	2.209(4)	Mn(5)-O(28)	2.238(4)	Mn(7)-O(37)	2.194(4)
Mn(3)-O(1)	1.833(3)	Mn(4)-O(17)	1.835(3)	Mn(9)-O(33)	1.842(3)
Mn(3)-O(14)	1.977(4)	Mn(4)-O(27)	1.967(4)	Mn(9)-O(38)	1.975(4)
Mn(3)-O(8)	1.978(4)	Mn(4)-O(21)	1.964(4)	Mn(9)-O(48)	1.984(4)
Mn(3)-O(4)	1.997(4)	Mn(4)-O(18)	1.990(4)	Mn(9)-O(36)	1.983(4)
Mn(3)-O(6)	2.182(4)	Mn(4)-O(23)	2.179(4)	Mn(9)-O(46)	2.190(4)
Mn(3)-O(16)	2.224(4)	Mn(4)-O(25)	2.230(4)	Mn(9)-O(40)	2.206(4)
Mn(2)-Mn(1)	3.430	Mn(5)-Mn(6)	3.452	Mn(7)-Mn(8)	3.427
Mn(2)-Mn(3)	3.438	Mn(5)-Mn(4)	3.442	Mn(7)-Mn(9)	3.459
Mn(1)-Mn(3)	3.264	Mn(4)-Mn(6)	3.259	Mn(8)-Mn(9)	3.266
Angles					
O(1)-Mn(1)-O(11)	95.4(2)		O(1)-Mn(1)-O(5)	95.1(2)	
O(11)-Mn(1)-O(5)	169.4(2)		O(1)-Mn(1)-O(2)	176.2(2)	
O(11)-Mn(1)-O(2)	84.4(2)		O(5)-Mn(1)-O(2)	85.2(2)	
O(1)-Mn(1)-O(7)	91.8(2)		O(11)-Mn(1)-O(7)	85.3(2)	
O(5)-Mn(1)-O(7)	95.8(2)		O(2)-Mn(1)-O(7)	84.34(14)	
O(1)-Mn(1)-O(9)	97.9(2)		O(11)-Mn(1)-O(9)	90.9(2)	
O(5)-Mn(1)-O(9)	86.2(2)		O(2)-Mn(1)-O(9)	85.93(14)	
O(7)-Mn(1)-O(9)	169.84(14)		O(3)-Mn(2)-O(12)	90.1(2)	
O(3)-Mn(2)-O(15)	79.19(14)		O(12)-Mn(2)-O(15)	94.5(2)	
O(3)-Mn(2)-O(1)	172.49(14)		O(12)-Mn(2)-O(1)	87.78(14)	
O(15)-Mn(2)-O(1)	93.78(14)		O(3)-Mn(2)-O(10)	87.09(14)	
O(12)-Mn(2)-O(10)	93.0(2)		O(15)-Mn(2)-O(10)	164.4(2)	
O(1)-Mn(2)-O(10)	100.21(14)		O(3)-Mn(2)-O(13)	93.5(2)	
O(12)-Mn(2)-O(13)	173.3(2)		O(15)-Mn(2)-O(13)	91.7(2)	
O(1)-Mn(2)-O(13)	89.31(14)		O(10)-Mn(2)-O(13)	81.6(2)	
O(1)-Mn(3)-O(14)	94.5(2)		O(1)-Mn(3)-O(8)	95.6(2)	
O(14)-Mn(3)-O(8)	169.6(2)		O(1)-Mn(3)-O(4)	175.6(2)	
O(14)-Mn(3)-O(4)	83.9(2)		O(8)-Mn(3)-O(4)	86.2(2)	
O(1)-Mn(3)-O(6)	91.58(14)		O(14)-Mn(3)-O(6)	88.6(2)	
O(8)-Mn(3)-O(6)	93.6(2)		O(4)-Mn(3)-O(6)	84.34(14)	
O(1)-Mn(3)-O(16)	101.12(14)		O(14)-Mn(3)-O(16)	93.1(2)	
O(8)-Mn(3)-O(16)	82.5(2)		O(4)-Mn(3)-O(16)	83.04(14)	
O(6)-Mn(3)-O(16)	167.00(13)		Mn(3)-O(1)-Mn(1)	125.0(2)	
Mn(3)-O(1)-Mn(2)	118.0(2)		Mn(1)-O(1)-Mn(2)	117.0(2)	
O(17)-Mn(4)-O(21)	95.3(2)		O(17)-Mn(4)-O(27)	94.6(2)	
O(21)-Mn(4)-O(27)	169.7(2)		O(17)-Mn(4)-O(18)	176.4(2)	
O(21)-Mn(4)-O(18)	85.8(2)		O(27)-Mn(4)-O(18)	84.5(2)	
O(17)-Mn(4)-O(23)	92.0(2)		O(21)-Mn(4)-O(23)	94.6(2)	
O(27)-Mn(4)-O(23)	87.9(2)		O(18)-Mn(4)-O(23)	84.50(14)	
O(17)-Mn(4)-O(25)	100.2(2)		O(21)-Mn(4)-O(25)	82.7(2)	
O(27)-Mn(4)-O(25)	92.8(2)		O(18)-Mn(4)-O(25)	83.33(14)	
O(23)-Mn(4)-O(25)	167.69(14)		O(26)-Mn(5)-O(29)	96.6(2)	

O(26)-Mn(5)-O(19)	79.27(14)	O(29)-Mn(5)-O(19)	93.3(2)
O(26)-Mn(5)-O(17)	94.44(14)	O(29)-Mn(5)-O(17)	86.90(14)
O(19)-Mn(5)-O(17)	173.69(14)	O(26)-Mn(5)-O(31)	162.4(2)
O(29)-Mn(5)-O(31)	91.0(2)	O(19)-Mn(5)-O(31)	84.53(14)
O(17)-Mn(5)-O(31)	101.77(14)	O(26)-Mn(5)-O(28)	92.1(2)
O(29)-Mn(5)-O(28)	170.0(2)	O(19)-Mn(5)-O(28)	93.2(2)
O(17)-Mn(5)-O(28)	87.45(14)	O(31)-Mn(5)-O(28)	82.1(2)
O(17)-Mn(6)-O(30)	95.1(2)	O(17)-Mn(6)-O(24)	94.7(2)
O(30)-Mn(6)-O(24)	170.0(2)	O(17)-Mn(6)-O(20)	177.7(2)
O(30)-Mn(6)-O(20)	85.6(2)	O(24)-Mn(6)-O(20)	84.7(2)
O(17)-Mn(6)-O(32)	97.8(2)	O(30)-Mn(6)-O(32)	87.9(2)
O(24)-Mn(6)-O(32)	88.7(2)	O(20)-Mn(6)-O(32)	84.43(14)
O(17)-Mn(6)-O(22)	92.2(2)	O(30)-Mn(6)-O(22)	85.3(2)
O(24)-Mn(6)-O(22)	96.4(2)	O(20)-Mn(6)-O(22)	85.59(14)
O(32)-Mn(6)-O(22)	168.3(2)	Mn(6)-O(17)-Mn(4)	124.6(2)
Mn(4)-O(17)-Mn(5)	118.2(2)	Mn(6)-O(17)-Mn(5)	117.1(2)
O(39)-Mn(7)-O(43)	96.6(2)	O(39)-Mn(7)-O(34)	79.8(2)
O(43)-Mn(7)-O(34)	91.8(2)	O(39)-Mn(7)-O(33)	91.59(14)
O(43)-Mn(7)-O(33)	86.96(14)	O(34)-Mn(7)-O(33)	171.2(2)
O(39)-Mn(7)-O(41)	164.2(2)	O(43)-Mn(7)-O(41)	91.9(2)
O(34)-Mn(7)-O(41)	86.6(2)	O(33)-Mn(7)-O(41)	102.15(14)
O(39)-Mn(7)-O(37)	89.9(2)	O(43)-Mn(7)-O(37)	172.6(2)
O(34)-Mn(7)-O(37)	92.8(2)	O(33)-Mn(7)-O(37)	89.38(14)
O(41)-Mn(7)-O(37)	82.6(2)	O(33)-Mn(8)-O(44)	94.8(2)
O(33)-Mn(8)-O(35)	178.0(2)	O(44)-Mn(8)-O(35)	85.7(2)
O(33)-Mn(8)-O(45)	94.5(2)	O(44)-Mn(8)-O(45)	169.9(2)
O(35)-Mn(8)-O(45)	85.2(2)	O(33)-Mn(8)-O(47)	93.7(2)
O(44)-Mn(8)-O(47)	87.8(2)	O(35)-Mn(8)-O(47)	84.40(14)
O(45)-Mn(8)-O(47)	95.4(2)	O(33)-Mn(8)-O(42)	98.2(2)
O(44)-Mn(8)-O(42)	88.5(2)	O(35)-Mn(8)-O(42)	83.76(14)
O(45)-Mn(8)-O(42)	86.4(2)	O(47)-Mn(8)-O(42)	167.8(2)
O(33)-Mn(9)-O(38)	94.8(2)	O(33)-Mn(9)-O(36)	176.3(2)
O(38)-Mn(9)-O(36)	82.4(2)	O(33)-Mn(9)-O(48)	97.0(2)
O(38)-Mn(9)-O(48)	168.2(2)	O(36)-Mn(9)-O(48)	85.8(2)
O(33)-Mn(9)-O(46)	90.7(2)	O(38)-Mn(9)-O(46)	89.5(2)
O(36)-Mn(9)-O(46)	86.91(14)	O(48)-Mn(9)-O(46)	90.6(2)
O(33)-Mn(9)-O(40)	98.1(2)	O(38)-Mn(9)-O(40)	95.4(2)
O(36)-Mn(9)-O(40)	84.54(14)	O(48)-Mn(9)-O(40)	82.7(2)
O(46)-Mn(9)-O(40)	169.52(14)	Mn(9)-O(33)-Mn(8)	124.8(2)
Mn(9)-O(33)-Mn(7)	118.5(2)	Mn(7)-O(33)-Mn(8)	116.6(2)

reasons, the Mn(2), Mn(5) and Mn(7) atoms can be assigned as the Mn^{II} center since all Mn(2,5,7)-O distances are longer than those for Mn^{III}-O, as expected for the lower oxidation state. A bond valence sum analysis was also calculated on complex **1b**, and the values are 3.07, 2.13, and 3.06 for Mn(1), Mn(2) and Mn(3), respectively. Bond valence sums for complex **1b** indicate that the oxidation state is trapped $Mn^{II}Mn^{III}_2$, where Mn(2) is found as Mn^{II} oxidation state and Mn(1) and Mn(3) are found as Mn^{III} oxidation states.

Magnetochemistry

The variable temperature dc magnetic susceptibility data was collected for microcrystalline samples of compounds **1** (mainly complex **1a** and minor product **1b** mixture) and **1a** in the temperature range of 2-310 K at a magnetic field of 10.0 kG. In Fig. 3 are given plots of the χ_m and $\chi_m T$ per molecule (emu·K/mol) vs. temperature. The value of $\chi_m T$ gradually decreases from 8.81 emu·K/mol and 9.05 emu·K/mol at 311 K to 0.63 emu·K/mol and 0.66 emu·K/mol at 2.0 K for compounds **1** and **1a**, respectively. The magnetic data for complexes **1** and **1a** are similar. These behaviors indicate weak antiferromagnetic interactions within the trinuclear complexes.

A theoretical expression for the molar paramagnetic susceptibility of a $Mn^{II}Mn^{III}_2$ complex can be derived, assuming isotropic exchange interactions and by using the spin

Hamiltonian in eq 1.

$$H = -2[J_{12}(S_1S_2) + J_{23}(S_2S_3) + J_{31}(S_3S_1)] \quad (1)$$

If it is assumed that the two Mn^{III} ions are equivalent, then there are two exchange parameters, $J_A = J_{12} = J_{13}$ for the Mn^{II}-Mn^{III} interactions and $J_B = J_{23}$ for the Mn^{III}-Mn^{III} interaction. Using this model, Vincent et al. have derived the formula expression of the molar paramagnetic susceptibility.[3] The best-fit J_A, J_B and g parameters for complex **1** are -4.98 cm^{-1}, -3.65 cm^{-1}, and 2.00, respectively. The best-fitting parameters predict that the first excited state S = 3/2 is 4.32 cm^{-1} higher energy than the S = 1/2 ground state, which is similar to the magnetic properties of complex **3**.[4] However, the J_A/J_B ratio of 1.36 for complex **1** is close to the value of 1.38 for complex **4**, where the ground state is either 1/2 or 3/2.[6] To confirm the magnetic susceptibility data have not been interrupted by the applied field, the AC magnetic measurements were conducted in a 2.0-242.6 K temperature range at a 1.0 G alternating field. The plots of the χ_m and $\chi_m T$ per molecule vs. temperature of DC (10.0 kG) and AC (1.0 G) data are shown in Fig. 4. The DC magnetic susceptibility data is consistent with the AC magnetic susceptibility data, indicating the DC applied field does not affect the magnetic susceptibility data.

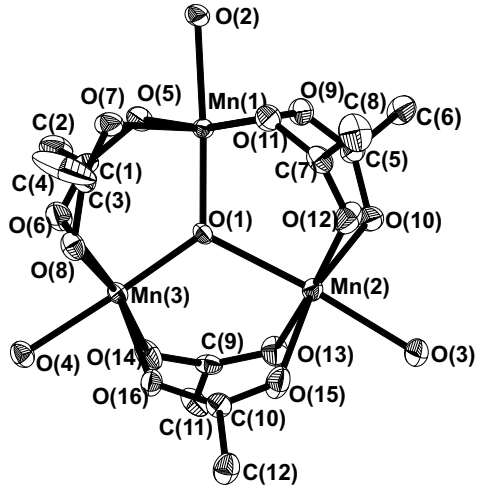

Fig. 2. Crystallographic Structure of $[Mn_3O(O_2CCCl_3)_6(H_2O)_3]\cdot 0.5C_6H_{14}$ (**1b**). Thermal ellipsoids at the 50% probability level. The Cl, H atoms and solvated molecules have been omitted for clarity.

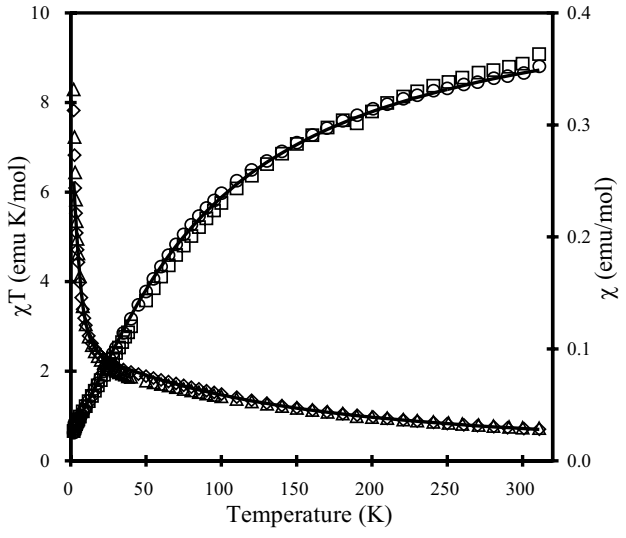

Fig. 3. Plots of χ_M and $\chi_M T$ vs temperature for complex **1** (◊, O) and complex **1a** (Δ, □). Data were collected in an applied field of 10.0 kG. The solid line results from a fit of the data to the appropriate theoretical equation: see the text for parameter.

The ground state of complex **1** is confirmed by magnetization measurements at 2.0 K up to a 70.0 kG field. For compounds **1** and **1a**, $M/N\beta$ values are 1.93 and 1.87, respectively. The results are plotted in Fig. 5 and the solid line (S = 3/2) and dashed line (S = 1/2) in the figure result from the Brillouin function.[14] The $M/N\beta$ values are greater for a pure S = 1/2 ground state but lower for a pure S = 3/2 ground state, which are inconsistent with an S =1/2 ground state and are close to the magnetization data of complex **4**.[6] A mixed ground state for complex **1** was observed. EPR experiments were carried out to support the conclusion from magnetic

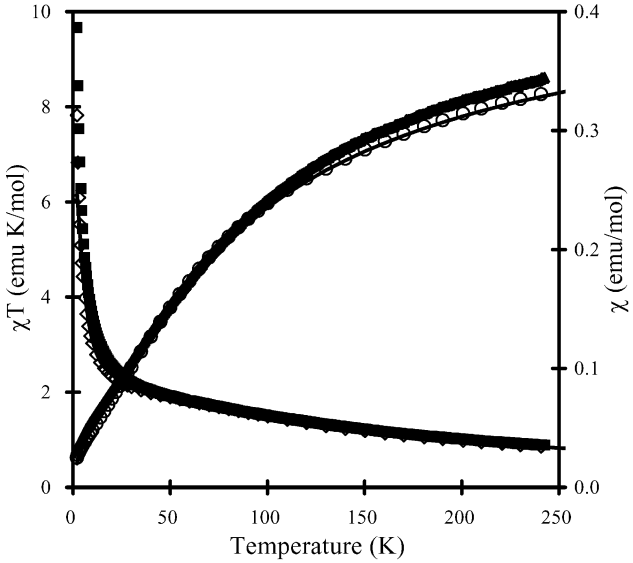

Fig. 4. Plots of χ_M and $\chi_M T$ vs temperature for complex **1** at 10.0 kG DC field (◊, O) and 1.0 G AC field (■, ▲).

measurements.

EPR spectra

EPR spectroscopy is very practical in studying the ground state of polynuclear manganese complexes with half-integer spin states. In general, for complexes with an S = 3/2 ground state, there is a strong signal in the g ≈ 4 region at low temperature, where intensity decreases with temperature

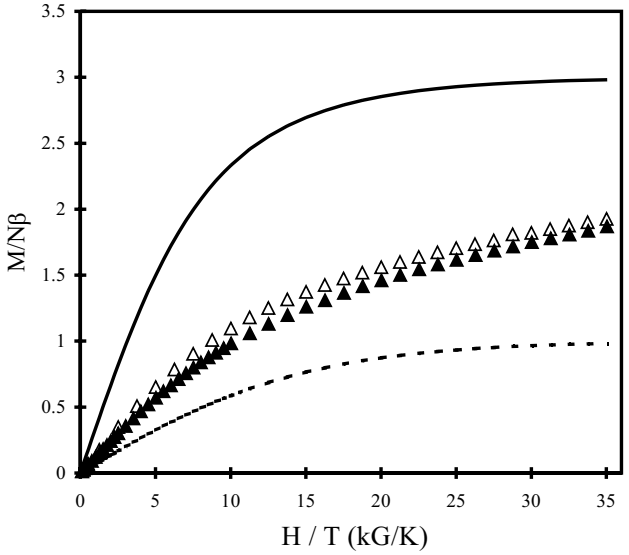

Fig. 5. Magnetization plots (M/Nβ) vs H/T (kG/K) for complex **1** (▲) and complex **1a** (Δ).

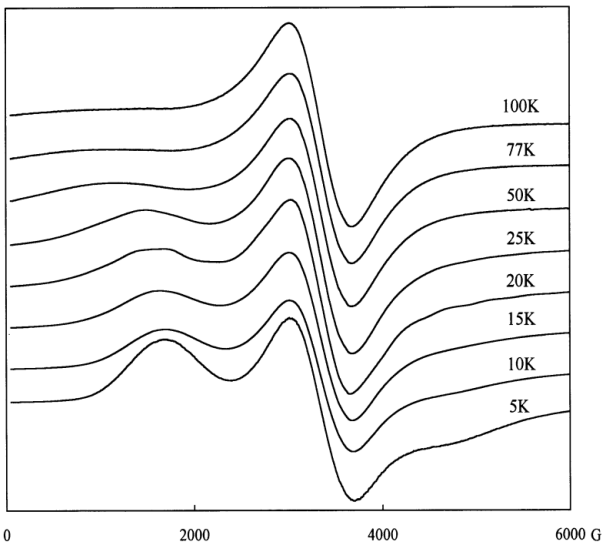

Fig. 6. Temperature dependence of the X-band EPR spectra of a polycrystalline sample of complex **1**.

increases, indicating a depopulation of this state as the temperature is increased. The X-band EPR spectra for a polycrystalline sample of complex **1** in the range of 5-100 K are shown in Fig. 6. The intensity of g ≈ 4 single decreases with increasing temperature, indicating depopulation of this state as the temperature is increased. These spectra clearly show that the ground state of complex has an S = 3/2. However, the bands centered at g ≈ 2 single are also present when the temperature decreases. These spectra clearly show that the ground state of complex **1** has a mixed ground, in agreement with the fit of magnetic susceptibility and magnetization measurement.

Supplementary Material

Crystallographic data for the structural analysis have been deposited with the Cambridge Crystallographic Data Centre under CCDC Nos. 201427 and 201426 for compounds **1a** and **1b**, respectively.

ACKNOWLEDGEMENT

We thank the National Science Council of the Republic of China for support.

Received April 21, 2003.

REFERENCES

1. Baikei, A. R. E.; Hursthouse, M. B.; New, D. B.; Thornton, P. *J. Chem. Soc., Chem. Commun.* **1978**, 62.
2. Baikei, A. R. E.; Hursthouse, M. B.; New, L.; Thornton, P.; White, R. G. *J. Chem. Soc., Chem. Commun.* **1980**, 684.
3. Vincent, J. B.; Chang, H.-R.; Folting, K.; Huffman, J. C.; Christou, G.; Hendrickson, D. N. *J. Am. Chem. Soc.* **1987**, *110*, 5703.
4. McCusker, J. K.; Jang, H. G.; Wang, S. Y.; Christou, G.; Hendrickson, D. N. *Inorg. Chem.* **1992**, *31*, 1874.
5. Zhang, S. W.; Wei, Y. G.; Liu, Q.; Shao, M. C.; Zhou, W. S. *Polyhedron* **1996**, *15*, 1041.
6. Ribas, J.; Albela, B.; Stoeckli-Evans, H.; Christou, G. *Inorg. Chem.* **1997**, *36*, 2352.
7. Zhong, Z. J.; Tao, J. T.; Li, H.; You, X. Z.; Mak, T. C. W. *Polyhedron* **1997**, *16*, 1719.
8. Wu, R.W.; Royraz, M.; Sowrey, F. E.; Anson, C. E.; Wocadlo, S.; Powell, A. K.; Jayasooriya, U. A.; Cannon, R. D.; Naknmoto, T.; Katada, M.; Sano, H. *Inorg. Chem*. **1998**,

37, 1913.
9. An, J.; Chen, Z. D.; Bian, J. A.; Jin, X. L.; Wang, S. X.; Xu, G. X. *Inorg. Chim. Acta* **1999**, *287*, 82.
10. Li, J.; Zhang, F. X.; Shi, Q. Z.; Wang, J.; Wang, Y.; Zhou, Z. Y. *Inorg. Chem. Commun.* **2002**, *5*, 51.
11. Lis, T. *Acta Crystallogr. B* **1980**, *36*, 2042.
12. Boudreaux, E. A.; Mulay, L. N. In *Theory and Application of Molecular Paramagnetism*; John Wiley & Sons: New York, 1976; p 491.
13. Brown, I. D.; Altermatt, D. *Acta Crystallogr. B* **1985**, *41*, 244.
14. Carlin, R. L. In *Magnetochemistry*; Springer-Verlag: New York, 1986; pp 16-17.